

Heavy Neutrino Search via Semileptonic Higgs Decay at the LHC

Arindam Das,^{1,2,3,*} Yu Gao,^{4,5,†} and Teruki Kamon^{6,‡}

¹*School of Physics, KIAS, Seoul 02455, Korea*

²*Department of Physics & Astronomy,*

Seoul National University 1 Gwanak-ro, Gwanak-gu, Seoul 08826, Korea

³*Korea Neutrino Research Center, Bldg 23-312,*

Seoul National University, Sillim-dong, Gwanak-gu, Seoul 08826, Korea

⁴*Key Laboratory of Particle Astrophysics, Institute of High Energy Physics,
Chinese Academy of Sciences, Beijing, 100049, China*

⁵*Department of Physics and Astronomy,*

Wayne State University, Detroit, 48201, USA

⁶*Mitchell Institute for Fundamental Physics and Astronomy,
Department of Physics and Astronomy,*

Texas A&M University, College Station, TX 77843-4242, USA

Abstract

In the inverse see-saw model the effective neutrino Yukawa couplings can be sizable due to a large mixing angle between the light (ν) and heavy neutrinos (N). When the right handed neutrino (N) can be lighter than the Standard Model (SM) Higgs boson (h). It can be produced via the on-shell decay of the Higgs, $h \rightarrow N\nu$ at a significant branching fraction at the LHC. In such a process N mass can be reconstructed in its dominant $N \rightarrow W\ell$ decays. We perform an analysis on this channel and its relevant backgrounds, among which the W +jets background is the largest. Considering the existing mixing constraints from the Higgs and electroweak precision data, the best sensitivity of the heavy neutrino search is achieved for benchmark N mass at 100 and 110 GeV for upcoming high luminosity LHC runs.

PACS numbers:

Keywords: Heavy Neutrino Search, Higgs boson Data, New Production Channel, Collider Phenomenology

*Electronic address: arindam@kias.re.kr

†Electronic address: gaoyu@ihep.ac.cn

‡Electronic address: kamon@physics.tamu.edu

I. INTRODUCTION

The current experimental results on the neutrino oscillation phenomena [1], including the recent measurements of the so-called reactor angle [2–7], have established the existence of neutrino masses and flavor mixings, which require us to extend the Standard Model (SM). The seesaw extension of the SM [8–14] is probably the simplest idea for explaining the very small neutrino masses naturally, where the SM-singlet heavy right-handed Majorana neutrinos induce the dimension five operators leading to very small Majorana neutrino masses (the seesaw mechanism [8–14]). The seesaw scale varies from the intermediate scale to the electroweak scale as we change the neutrino Dirac Yukawa coupling (Y_D) from the scale of top quark Yukawa coupling ($Y_D \sim 1$) to the scale of electron Yukawa coupling ($Y_D \sim 10^{-6}$).

In high energy collider experimental point of view, it is interesting if the heavy neutrino mass lies at the TeV scale or smaller, because such heavy neutrinos could be produced at high energy colliders, such as the Large Hadron Collider (LHC) and the Linear Collider (LC) being projected as energy frontier physics in the future. However, since the heavy neutrinos are singlet under the SM gauge group, they obtain the couplings with the weak gauge bosons only through the mixing via the Dirac Yukawa coupling. For the seesaw mechanism at the TeV scale or smaller, the Dirac Yukawa coupling is too small ($Y_D \sim 10^{-6} - 10^{-5}$) to produce the observable amount of the heavy neutrinos at the colliders.

There is another type of seesaw mechanism so-called the inverse seesaw [15, 16], where the small neutrino mass is obtained by tiny lepton-number-violating parameters, rather than the suppression by the heavy neutrino mass scale in the ordinary seesaw mechanism. In the inverse seesaw scenario, the heavy neutrinos are pseudo-Dirac particles and their Dirac Yukawa couplings with the SM lepton doublets and the Higgs doublet can be even order one, while reproducing the small neutrino masses. Thus, the heavy neutrinos in the inverse seesaw scenario can be produced at the high energy colliders through the sizable mixing with the SM neutrinos.

Since any number of singlets can be added to a gauge theory without introducing anomalies, one could exploit this freedom to find a natural alternative low-scale realization of the seesaw mechanism. In the low scale seesaw ¹, the SM is extended by n_1 SM singlet RHNs N_R and n_2 sterile neutrinos S . For the simplicity we consider a basis where the charged

¹ Apart from the canonical seesaw mechanism, there are other simple scenarios like type-II and type-III models which describe the generation of the neutrino mass, a detailed study has been given in [17].

leptons are identified with their mass eigenstates. Hence before the electroweak symmetry breaking (EWSB) we write the general interaction Lagrangian as

$$\begin{aligned}
-\mathcal{L}_{int} &= Y_1 \bar{\ell}_L H N_R + Y_2 \bar{\ell}_L H S + M_N \bar{N}_R^c S + \frac{1}{2} \mu \bar{S}^c S + \\
&+ \frac{1}{2} M_R \bar{N}_R^c N_R + h.c.
\end{aligned} \tag{1}$$

where ℓ_L and H are the SM lepton and Higgs doublets, respectively. Y_1 and Y_2 are the Yukawa coupling matrices of dimensions $3 \times n_1$ and $3 \times n_2$ respectively. M_R and μ are Majorana mass matrices for N_R and S of dimensions $n_1 \times n_1$ and $n_2 \times n_2$, respectively. Due to the presence of μ and M_R mass parameters the lepton number is broken. After the EWSB breaking, from Eq. 1 we get

$$\begin{aligned}
-\mathcal{L}_{mass} &= M_D \bar{\nu}_L N_R + M \bar{\nu}_L S + M_N \bar{N}_R^c S + \frac{1}{2} \mu \bar{S}^c S \\
&+ \frac{1}{2} M_R \bar{N}_R^c N_R + h.c.
\end{aligned} \tag{2}$$

where $M_D = Y_1 \frac{v}{\sqrt{2}}$, $M = Y_2 \frac{v}{\sqrt{2}}$ and $\langle H \rangle = \frac{v}{\sqrt{2}}$. Hence the neutral fermion mass matrix can be written as

$$-\mathcal{L}_{mass} = \frac{1}{2} \begin{pmatrix} \bar{\nu}_L & \bar{N}_R^c & \bar{S}^c \end{pmatrix} \begin{pmatrix} 0 & M_D & M \\ M_D^T & M_R & M_N \\ M^T & M_N^T & \mu \end{pmatrix} \begin{pmatrix} \nu_L^c \\ N_R \\ S \end{pmatrix}. \tag{3}$$

From Eq. 3 we can get a variety of the seesaw scenarios by setting respective terms to be zero². The simplest scenario is the inverse seesaw [15, 16] model which has been studied in [18, 19] using vacuum stability and fitting the neutrino oscillation data considering M and M_R to be zero [15, 16]. Sub-matrices M_N and μ did not arrive from the $SU(2)_L$ symmetry breaking whereas μ is the lepton number violating mass term. Hence they might follow the hierarchy $M_N \gg M_D \gg \mu$. The value of μ can be small by 't Hooft's naturalness criteria [20] since the expected degree of lepton number violation becomes naturally small. In a common scenario each of M_N , M_D and μ are 3×3 matrices (See, Ref. [21] where a minimal scenario has been studied. In this article we consider a minimal scenario where two generations of the RHNs are involved such a scenario can satisfy the neutrino oscillation data. The effective light neutrino mass matrix can be written under the seesaw approximation as

$$M_\nu^{\text{light}} \sim M_D (M_N^T)^{-1} \mu M_N^{-1} M_D^T \tag{4}$$

² Simply assigning the lepton numbers for the SM singlet RHNs N_R and S as +1 and -1, respectively a purely inverse seesaw scenario can be achieved where the (13), (22) and (31) elements of the Eq. 3 will not arise.

where as in the heavy sector we will have the three pairs of degenerate pseudo-Dirac neutrinos of masses of order $M_N \mp \mu$. The smallness of M_ν^{light} is naturally obtained from both of the smallness of μ and $\frac{M_D}{M_N}$. Hence $M_\nu^{\text{light}} \sim \mathcal{O}(0.1)$ eV can be obtained from $\frac{M_D}{M_N} \sim 0.01$ and $\mu \sim \mathcal{O}(100)$ eV. Thus the seesaw scale can be lowered considering $Y_1 \sim \mathcal{O}(0.1)$ which implies $M_D \sim 10$ GeV and $M_N \sim 1$ TeV. The inverse seesaw scenario has also been discussed in the supersymmetric context in Ref.[22] (and also the references there in). The inverse seesaw scenario has been discussed under the general parametrization in [23] using Casas-Ibarra conjecture for general Y_D . In [25, 26] the Casas- Ibarra parametrization has been used to study the inverse seesaw scenario. A generalized scenario of the inverse seesaw has been discussed under the left-right scenario has been discussed in Ref. [24]).

We rather simplify the scenario a bit further with respect to [19]. In a simplified scenario M_D and M_N can be the diagonal matrices where as the flavors are encoded in the μ matrix. This is called the Flavor Diagonal (FD) scenario. Explicit numerical fits are also given in [23] using the neutrino oscillation data, non-unitarity effects and lepton flavor violation measurements. In the collider analysis we consider a minimal set up where both of M_N are proportional to the 2×2 unit matrix ($\mathbf{1}_{2 \times 2}$) where the entire flavor mixing structure lies in μ which is another 2×2 matrix keeping Y_D as a diagonal matrix proportional to $\mathbf{1}_{2 \times 2}$. Such a scenario can also reproduce the neutrino oscillation data. It means that there are two degenerate generations of each of N_R and S whose mass can be considered at the TeV scale. Such a scenario has also been used in Ref.[23]. Such heavy neutrinos can be observed at the LHC from a variety of production processes [27]. We first study a model-independent search for high luminosity LHC runs and then interpret the search prospects with a benchmark FD inverse seesaw scenario. Due to flavor dependence in electroweak precision and Higgs decay constraints, we consider benchmark FD case in which both the first two flavor (electron and muon) heavy pseudo-Dirac pairs are at the TeV scale. Due to the degeneracy we consider that both of the electron and muon flavor RHNs (N) have the same mass, and their decays into electron and muons contribute to our collider signal.

For LHC production we focus on the $pp \rightarrow hj$ channel, where the Higgs boson subsequently decays as $h \rightarrow N\nu$ via the $Y_1 \bar{L} H N_R$ interaction term. The Higgs boson can be copiously produced by gluon fusion at the LHC, and due to its relatively narrow \sim MeV scale decay width, the Higgs boson decay branchings are more sensitively affected by the presence of a new $h \rightarrow N\nu$ channel, if compared to the decay of W, Z bosons. When N decay leptonically the $h \rightarrow 2l2\nu$ channel has been previously studied in [28, 32, 34], and here

we will examine the $h \rightarrow 2jl\nu$ channel from the semileptonic N decay, where a N mass peak is reconstructible in the final state. As we will discuss later, an associated jet is necessary for this Higgs decay channel both for event triggering and the SM background veto.

Our paper is arranged in the following way. In Sec. II we discuss the recent experimental bounds on the heavy neutrino searches. In Sec. III we discuss about the $h+j$ production and the decays of the Higgs boson into the heavy neutrino. In Sec. IV we focus on the semileptonic Higgs decay channel and study the LHC search. A model-independent constraint is derived on the heavy-active neutrino mixing angle, and we comment on its effectiveness in the Inverse Seesaw model. Then we conclude in Sec. V.

II. BOUNDS ON THE MIXINGS

Being the SM gauge singlets, the heavy mass eigenstate of neutrinos can interact with the W and Z bosons via its mixings into the SM neutrino. Due to such mixing, the SM neutrino flavor eigenstate (ν) can be expressed as a linear combination of the light (ν_m) and heavy (N_m) mass eigenstates,

$$\nu \simeq U_{\ell m} \nu_m + V_{\ell N} N_m, \quad (5)$$

where U is the 3×3 light neutrino mixing matrix being identical to the PMNS matrix at the leading order if we ignore the non-unitarity effects. Where as $V_{\ell N} \simeq m_D M_N^{-1}$ is the mixing between the SM neutrino and the SM gauge singlet heavy neutrino assuming $|V_{\ell N}| \ll 1$. The charged current (CC) and neutral current (NC) interactions can be expressed in terms of the mass eigenstates of the neutrinos as

$$\mathcal{L}_{CC} \supset -\frac{g}{\sqrt{2}} W_\mu \bar{e} \gamma^\mu P_L V_{\ell n} N_n + \text{h.c.}, \quad (6)$$

where e denotes the three generations of the charged leptons, and $P_L = \frac{1}{2}(1 - \gamma_5)$ is the projection operator. Similarly, in terms of the mass eigenstates the neutral current interaction is written as

$$\mathcal{L}_{NC} \supset -\frac{g}{2c_w} Z_\mu \left[\bar{N}_m \gamma^\mu P_L (V^\dagger V)_{mn} N_n + \{ \bar{\nu}_m \gamma^\mu P_L (U^\dagger V)_{mn} N_n + \text{h.c.} \} \right], \quad (7)$$

where $c_w = \cos \theta_w$ with θ_w being the weak mixing angle. We notice from Eqs. 6 and 7 that the production cross section of the heavy neutrinos at the high energy collider is proportional to $|V_{\ell N}|^2$. However, the Yukawa coupling in Eq. 1 can also be directly measured from the

decay mode of the Higgs boson such as $h \rightarrow N\nu$. The corresponding Yukawa coupling can be written as

$$\mathcal{L} \supset Y_D \frac{v}{\sqrt{2}} \bar{\nu}_L h N_R \quad (8)$$

using $\langle H \rangle = \begin{pmatrix} \frac{v+h}{\sqrt{2}} \\ 0 \end{pmatrix}$ where $V_{\ell N} = \frac{M_D}{M_N} = \frac{Y_D v}{\sqrt{2} M_N}$. Applying the bounds obtained from the invisible Higgs boson decay widths we can measure the allowed parameter regions for Y_D and $V_{\ell N}$. The recent and the projected bounds on the mixing angle as a function of M_N from different experiments are shown in Figs. 1 and 2.

For $M_N < M_Z$, the RHN can be produced from the Z -decay through through the NC interaction with missing energy. The heavy neutrino can decay according CC and NC interactions. Such processes have been discussed in [29–31]. In [31–34], a scale dependent production cross section at the Leading Order (LO) and Next-to-Leading-Order QCD (NLO QCD) of $N\nu$ at the LO and NLO have been studied at the 14 TeV LHC and 100 TeV hadron collider.

The L3 collaboration [35] has performed a search on such heavy neutrinos directly from the LEP data and found a limit on $\mathcal{B}(Z \rightarrow \nu N) < 3 \times 10^{-5}$ at the 95% CL for the mass range up to 93 GeV. The exclusion limits from $L3$ are given in Figs. 1 and 2 where the red dashed line stands for the limits obtained from e ($L3 - e$) in Fig. 1 and the red dotted line stands for the exclusion limits coming from μ ($L3 - \mu$) in Fig. 2.

The corresponding exclusion limits on $|V_{(\ell=e)N}|^2$ at the 95% CL [36, 37] have been drawn from the LEP2 data in Figs. 1. This is denoted by the dark magenta line. In this analysis they searched for $80 \text{ GeV} \leq M_N \leq 205 \text{ GeV}$ with a center of mass energy between 130 GeV to 208 GeV [37]. The LEP2 [37] has studied the $e^+e^- \rightarrow N\nu$ process followed by the $N \rightarrow eW$ mode to study the bounds on the corresponding mixing angle involved in the analysis. The bounds denoted by LEP2 have been taken from [37] where the data collected with the L3 detector for 208 GeV center of mass energy.

The DELPHI collaboration [38] had also performed the same search from the LEP-I data which set an upper limit for the branching ratio $\mathcal{B}(Z \rightarrow N\nu)$ about 1.3×10^{-6} at 95% CL for $3.5 \text{ GeV} \leq M_N \leq 50 \text{ GeV}$. Outside this range the limit starts to become weak with the increase in M_N . In both of the cases they have considered $N \rightarrow W\ell$ and $N \rightarrow Z\nu$ decays after the production of the heavy neutrino was produced. The exclusion limits for $\ell = e$ and μ are depicted by the blue dotted (dashed) lines for $e(\mu)$ in Fig. 1 (2).

The heavy neutrinos can participate in many electroweak (EW) precision tests due to the active-sterile couplings. For comparison, we also show the 95% CL indirect upper limit on the mixing angle, $|V_{\ell N}| < 0.030$ and 0.041 for $\ell = e$ (μ) respectively derived from a global fit to the electroweak precision data (EWPD), which is independent of M_N for $M_N > M_Z$, as shown by the horizontal purple dot-dashed (dashed) lines respectively in Fig. 1 (2) [40–42]. For the mass range, $M_N < M_Z$, it is shown in [43] that the exclusion limit on the mixing angle remains almost unaltered, however, it varies drastically at the vicinity of $M_N = 1$ GeV. For the flavor universal case the bound on the mixing angle is given as $|V_{\ell N}|^2 = 0.025$ from [40] which has been depicted in Figs. 1 and 2 with a purple solid line. Improvements in the EWPD has been observed in [39] for the general seesaw and three extra heavy neutrino cases. The 2σ bound allowed for $|V_{eN}|^2$ is below 2.5×10^{-3} for the lepton flavor conserving case for the general seesaw described by [39] and the bound for $|V_{\mu N}|^2$ is 4.4×10^{-4} . In the three extra heavy neutrino case the $2 - \sigma$ bound is shown as the same for the general seesaw case irrespective of the neutrino mass hierarchies. Where as the bounds on $|V_{\mu N}|^2$ for the NH case is $< 4.0 \times 10^{-4}$. That for the IH case is $< 5.3 \times 10^{-4}$. These limits are all under good agreement with the parameter spaces shown for the different mixing matrix elements applied in [23] for the inverse seesaw and calculated in [44] for the seesaw cases with appropriate general parametrization.

The relevant 95% CL upper limits are also shown to compare with the experimental bounds using the LHC Higgs boson data in [28] (also see, [27]) using the $2\ell 2\nu$ final state from the WW^* data at the LHC [45–49] for $\ell = e$ and μ combined. In this case $h \rightarrow N\nu, N \rightarrow W\ell, W \rightarrow \ell\nu$ ($h \rightarrow N\nu, N \rightarrow Z\nu, Z \rightarrow 2\ell$) mode has been considered to probe the mixing in [27, 28]. The darker green solid line named Higgs boson shows the relevant bounds on the mixing angle in Figs. 1 and 2. In this analysis we will compare our results taking this line as one of the references. We have noticed that the $|V_{\ell N}|^2$ can be as low as 4.86×10^{-4} while $M_N = 60$ GeV and the bound becomes stronger at $M_N = 100$ GeV as 3.73×10^{-4} . When $M_N > 100$ GeV, the bounds on $|V_{\ell N}|^2$ become weaker.

LHC has also performed the direct searches on the Majorana heavy neutrinos. The ATLAS detector at the 7 TeV with a luminosity of 4.9 fb^{-1} [50] studied the $\mu^\pm \mu^\pm + \text{jets}$ in the type-I seesaw model framework for $100 \text{ GeV} \leq M_N \leq 500 \text{ GeV}$. They performed the analyses at the 8 TeV LHC with a luminosity of 20.3 fb^{-1} in [51] and interpreted the limit in terms of the mixing angle, $|V_{\mu N}|^2$ which is shown in the Fig. 2. The corresponding bounds

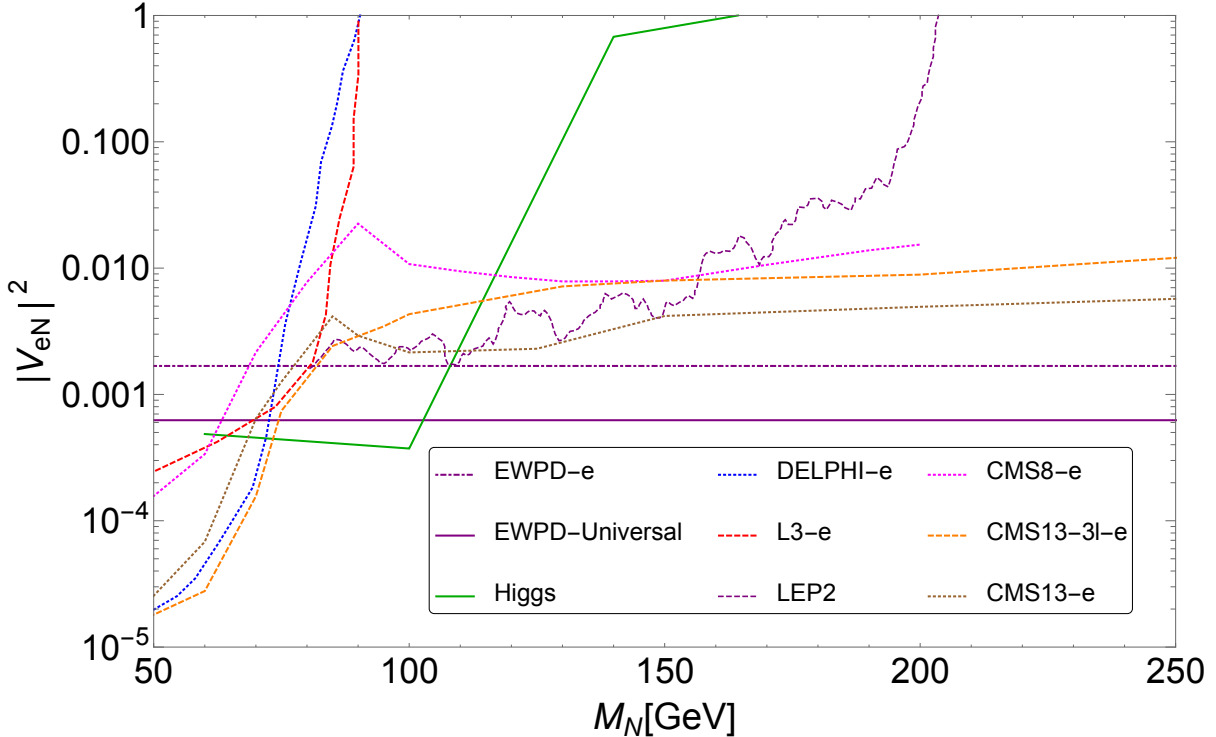


FIG. 1: Experimental upper bounds on $|V_{eN}|^2$ as a function of M_N .

for the μ are shown by the dashed orange line and marked as ATLAS8- μ in Fig. 2³.

The CMS also studied the type-I seesaw model from the $e^\pm e^\pm + \text{jets}$ and $\mu^\pm \mu^\pm + \text{jets}$ final states in [52] at the 8 TeV LHC with a luminosity of 19.7 fb^{-1} with $30 \text{ GeV} \leq M_N \leq 500 \text{ GeV}$. The limits from the CMS in the for μ is roughly comparable to the DELPHI result while $M_N < 70 \text{ GeV}$. The CMS limits are denoted by CMS8- μ and CMS8- e with the magenta dashed and dotted lines respectively in Fig. 2. The prospective high luminosity limits have been shown in [44, 53]. In Eq. 7, there is a part where the heavy neutrino can be produced in a pair from the NC interaction where the production cross section will be proportional to $|V_{\ell N}|^4$. The corresponding limits for the electrons are given in Fig. 1. The 8 TeV limits for the muons (electrons) are denoted as CMS8- μ (CMS8- e).

A detailed scale dependent LO and NLO-QCD studies of this process followed by various multi-lepton decays of the heavy neutrino have been studied in [54]. It is shown that $95 \text{ GeV} \leq M_N \leq 160 \text{ GeV}$ could be probed well at the high energy colliders at very high luminosity while the results will be better than the results from EWPD.

The updated limits at the 13 TeV LHC with a luminosity of 35.9 fb^{-1} have been shown

³ The weaker bounds of the 7 TeV ATLAS results are not shown in Fig. 2, however, the bounds can be read from [50].

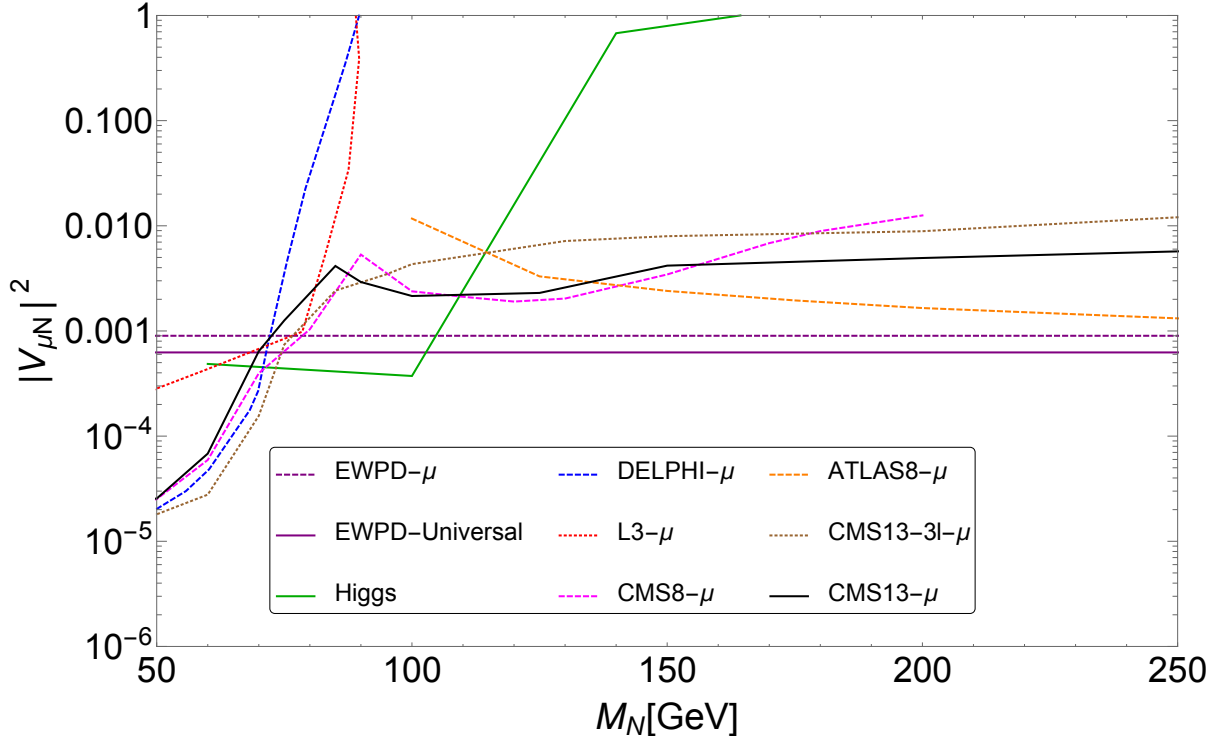


FIG. 2: Experimental upper bounds on $|V_{\mu N}|^2$ as a function of M_N .

in Fig. 1 and 2 from [55] for electron and muon respectively. The corresponding limit for the e (μ) is shown by the black dotted (dashed) line which marked as CMS13- e (CMS13- μ). Recently the CMS has performed the trilepton search from the Majorana RHNs [56] at the 13 TeV LHC with a luminosity of 35.9 fb^{-1} . The corresponding bounds for the e (μ) flavors are shown by the brown dotted (dashed) lines which are marked with CMS13- 3ℓ - e (CMS13- 3ℓ - μ).

In this work we consider the heavy neutrino from the on-shell decay of the Higgs boson. Therefore we choose ‘benchmark’ heavy neutrino masses below the Higgs boson mass, and adopt the experimental bounds on the mixing angles to forecast a maximally allowed production rate. We also give the production rates for a generic range of the mixing $|V_{\ell N}|^2 = 10^{-3}$ to 10^{-8} that are relevant to the current and prospective bounds.

III. HIGGS BOSON + JET CROSS-SECTIONS

The Higgs boson can decay into a right handed pseudo-Dirac heavy neutrino and a SM neutrino via the $\nu - N$ mixing. If M_N lies below the Higgs boson mass, the Higgs boson can decay on-shell into the heavy neutrino through a single production channel shown in Fig. 3.

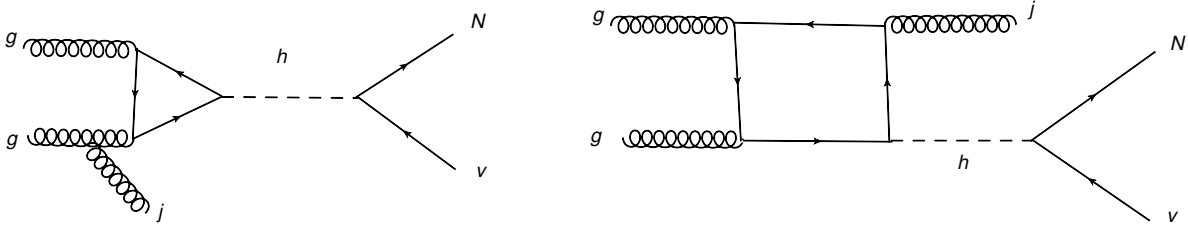


FIG. 3: Production processes of the heavy neutrino via Higgs boson decay with one associated jet. The extra jet originates from either the initial state or part of the hard process.

The Higgs boson's SM decay width is taken as $\Gamma_h^{\text{SM}} = 4.1$ MeV, with allowance to fit in BSM physics where the Higgs boson can decay into the SM singlet heavy neutrino in association with missing energy. The partial decay width is given by

$$\Gamma(h \rightarrow N\nu) = \frac{Y_N^2}{8\pi m_h^3} (m_h^2 - M_N^2)^2 \quad (9)$$

and it sums $h \rightarrow N\bar{\nu}$ and $h \rightarrow \bar{N}\nu$ cases. The branching fraction of the Higgs boson to each heavy neutrino is ⁴

$$\mathcal{B}_{h \rightarrow N\nu} = \frac{\Gamma(h \rightarrow N\nu)}{\Gamma_h^{\text{SM}} + \Gamma(h \rightarrow N\nu)} \quad (10)$$

We focus on the signal channel of single Higgs boson production with an associated jet, and utilize the consequent decay of the Higgs boson. The inclusion of an extra jet is necessary due to the requirement of experimentally triggering on the event, and also due to the fact that most of the Higgs boson decay products are not very energetic without a transverse boost from the associated initial state jet.

The search channel $pp \rightarrow hj$ needs a large p_T jet as event trigger and to reduce the amount of the SM background. Due to a large jet p_T , the hj production is generated at one-loop with a next-to-leading order model, see Section IV for details. Including the Higgs boson decay branching ratios, the signal cross-section for a single heavy neutrino can be written as

$$\sigma = \sigma(h + j)\mathcal{B}_{h \rightarrow N\nu}, \quad (11)$$

where the Higgs boson decay branching fraction $\mathcal{B}_{h \rightarrow N\nu}$ depends upon M_N and the size of $|V_{lN}|^2$. For each m_N , we will consider the current experimental bounds on $|V_{lN}|^2$ and use the

⁴ In the FD case, there are two heavy neutrinos and the total branching fraction is $\mathcal{B}_{h \rightarrow N\nu} = \frac{2\Gamma(h \rightarrow N\nu)}{\Gamma_h^{\text{SM}} + 2\Gamma(h \rightarrow N\nu)}$

maximal experimentally allowed $\mathcal{B}_{h \rightarrow N\nu}$ for the optimal signal rate. The maximally allowed production cross section is shown in Fig. 4 at 13 TeV LHC, with the requirement of the leading jet $p_T^j > 200$ GeV.

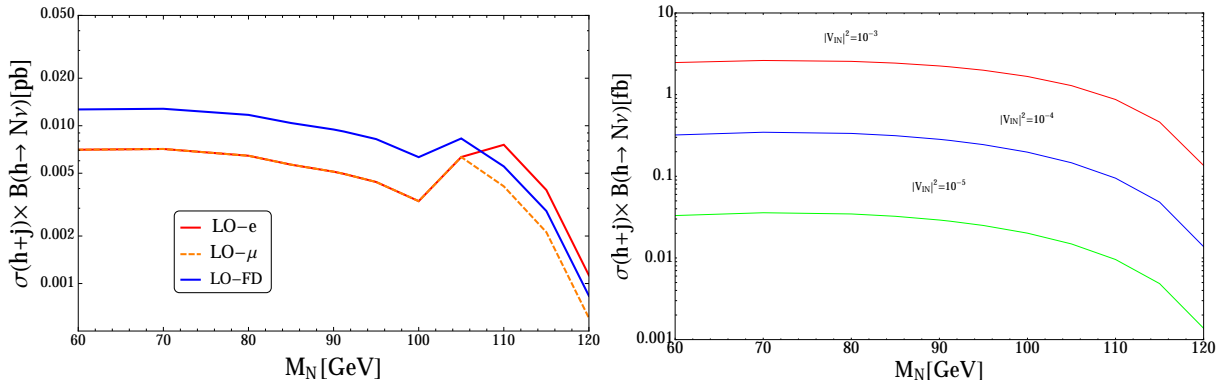


FIG. 4: Upper bounds on the leading-order production cross sections of $N\nu$ from $h + j$ process with maximally allowed mixing angles, with $p_T^j > 200$ GeV at $\sqrt{s} = 13$ TeV. The electron and muon flavor curves deviate due to different EWPD and LHC constraints. The right panel shows the single-flavor signal cross-section at fixed mixing angle values. For the FD case, the signal cross-section doubles as two flavors can contribute.

To calculate the prospective cross section in this channel, we consider the experimental mixing angles constraint from leptonic Higgs channel, as discussed in [27, 28]. While the Higgs boson bound is most stringent in a large N mass range, at N mass between 100-110 GeV, the EWPD bound [40] becomes stronger. We use the stronger of the two constraints to produce an upper bound of $|V_{lN}|^2$, and the heavy neutrino production cross section for the $h + j$ channel.

For the convenience of estimating generic signal rates, we also show the signal cross sections at fixed mixing angle values in Fig. 4. Note that $|V_{eN}|^2 = 10^{-5}$ will be nearly $\mathcal{O}(1)$ magnitude below the constraint obtained in [27, 28, 40] in case only a single lepton flavor considered. Note that The FD case for the ‘benchmark’ mixing angles can be nearly twice as large as the corresponding single flavor cases.

The produced heavy neutrino will then decay via the SM weak bosons such as W , Z (and h for heavier N). The corresponding decay widths are given in [23, 31]. N lighter than W and Z bosons will decay into three-body channels through the virtual W and Z bosons. The corresponding partial decay widths are given in [58, 59]. Note that the W channel will typically dominate both two-body decay, shown in Fig. 5. In our analysis, we require the reconstruction of both dijet mass at M_W and $lj\bar{j}$ invariant mass at M_N to veto against SM

backgrounds. Note the ljj system's mass window cut is M_N dependent, and should be tried for each choice of the M_N in the relevant parameter range. In case of a signal, if present, the determination of M_N may either come from M_{ljj} reconstruction or more sophisticated M_N -dependent template fits on the final state kinematics.

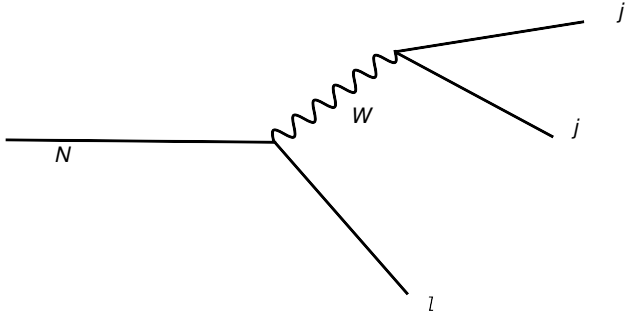


FIG. 5: Decay of the heavy neutrino in the ljj mode through the W boson.

IV. COLLIDER SIGNALS AND BACKGROUNDS

For successful triggering and background suppression, we require the leading jet p_T^j in $pp \rightarrow hj$ event to be at least 200 GeV. This jet is also more energetic than Higgs decay products and it assumes the role of triggering jet. At the same time, this jet transversely boosts the Higgs boson system so that the Higgs boson decay products acquire larger p_T^j and become more visible.

The Higgs boson then can decay into an $N - \nu$ pair. We focus on the $N \rightarrow ljj$ channel in which all three daughter particles are visible. The two jets from N arises from the on-shell decay of a W boson, so that their invariant mass would reconstruct to M_W . The lepton + dijet invariant mass would also reconstruct to M_N . These two invariant mass window cuts greatly suppress the SM backgrounds.

The after-cut cross-section is inferred from the $pp \rightarrow hj$ cross-section, decay branching ratios, and the selection efficiencies, as

$$\sigma = \sigma(hj)\mathcal{B}_{h \rightarrow N\nu}\mathcal{B}_{N \rightarrow ljj}A_{\text{eff}}. \quad (12)$$

For the selection efficiency A_{eff} , we consider the following detector-level cuts:

- (1) leading jet $p_T > 200$ GeV;
- (2) Additional two or more jets with $p_T > 30$ GeV and exactly one lepton with $p_T > 15$ GeV;

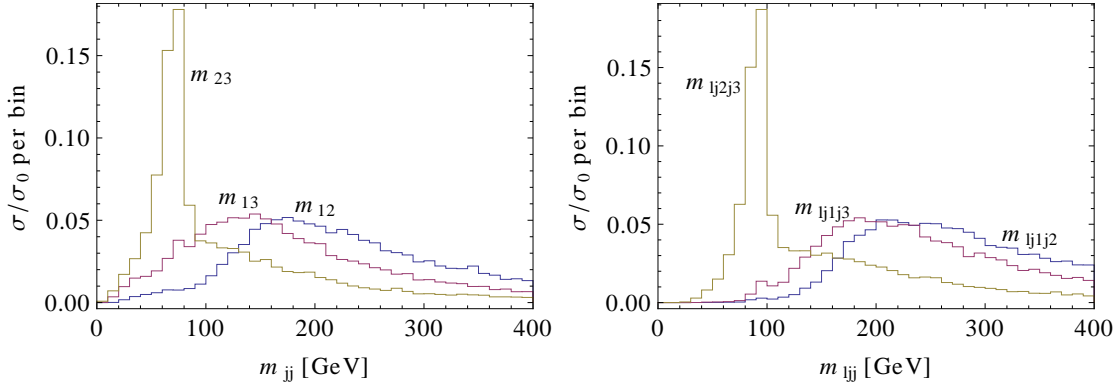


FIG. 6: Invariant dijet (left) and lepton+dijet (right) masses out of the three jets in signal events. N ($M_N = 100$ GeV) decay jets are mostly represented by j_2 and j_3 . In these histograms, the signal events only assume selection cuts $N_j \geq 3$ and $N_\ell \geq 1$.

- (3) $|M(j_2 j_3) - M_W| < 20$ GeV;
- (4) $|M(l_1 j_2 j_3) - M_N| < 20$ GeV;
- (5) $M_T(l_1 \cancel{E}) < 45$ GeV.

The selection cuts are designed to reconstruct the characteristic heavy neutrino mass as well as the physical W boson from N decay. These cuts are implemented at detector-level on Monte-Carlo simulated events. The leptons and jets pass basic detector pseudorapidity and p_T cuts (specified later), and they are ordered descendingly by p_T . The large leading jet p_T^j is important in suppressing weak boson + jets backgrounds. Vetoing a second lepton removes backgrounds with Z bosons. Here we focus on the hadronic W decay in order to reconstruct both the W boson and the N masses. These cuts greatly reduces SM backgrounds while retaining signal events at a much higher acceptance rate. Note that a fully leptonic decay of N can yield more leptons and suffer fewer SM background channels, but it also yields a neutrino and makes it impossible to reconstruct M_N .

Compared to the triggering jet, the N decay jets are mostly the second and third by p_T ordering. As illustrated in Fig. 6, an M_W peak is the most statistically pronounced between j_2 and j_3 among the three leading jets.

In the list of requirements, a few comments are due for the transverse mass M_T cut. After reconstructing the W and heavy neutrino N masses, significant SM background, esp. the W +jets channel, can still fake a heavy neutrino from a leptonically decayed W boson and two additional jets. To further remove such contamination, we make use of M_T of the

lepton and missing energy system, defined as,

$$M_T = \sqrt{2p_T^{\text{miss}} p_T^l (1 - \cos \Delta\phi)} \quad \text{as } \cancel{E}, l \text{ are massless.} \quad (13)$$

In signal events, l and \cancel{E} would originate from the limit mass gap between W and h bosons, while for Wj background they are from the physical W boson. This M_T nicely separates the signal and the leading Wj background, as illustrated in Fig. 7.

A number of the SM backgrounds are relevant for the $3j + \ell$ final state. The leading background channels typically arise from the presence of a W boson, from either direct production or top quark decay, along with extra jets. The leading background include W +jets, and top-quark producing channels. A large leading jet p_T is the most effective selection against the W +jets channel, but it would also suppress the signal rate. Top quark included backgrounds can be efficiently controlled by the N mass-window cut.

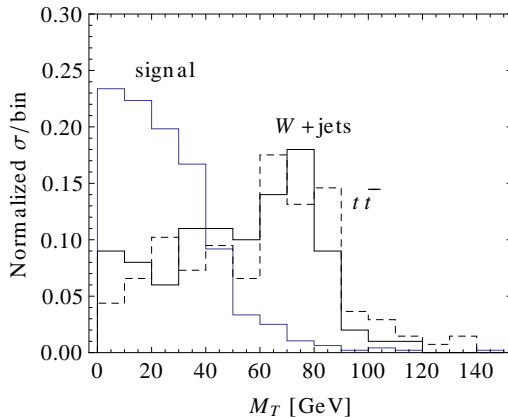


FIG. 7: The transverse mass can effectively separate semileptonic $h \rightarrow N\nu$ decay and a W decay, the latter being the leading SM Wj (solid) and $t\bar{t}$ (dashed) backgrounds. The cross-sections are normalized to better demonstrate the respective spectral shape. Here the heavy neutrino mass $m_N=110$ GeV.

In order to obtain the selection efficiencies we use the NLO model of the RHN as described in [31] and perform a 1-loop level simulation of $pp \rightarrow hj$ events with MadGraph5_aMC@NLO [60] code and its the Pythia-PGS package for event showering and detector simulation. Pile-up is not included. The 1-loop level calculation gives the leading-order cross-section for high jet- p_T Higgs production via gluon fusion. Additional jets and radiation are handled by Pythia. For a detector setup, we require a jet pseudo-rapidity $|\eta^j| < 2.5$, lepton pseudo-rapidity $|\eta^\ell| < 2.4$, minimal jet and lepton transverse momenta p_T^j and p_T^ℓ at 30 GeV and 15 GeV, respectively.

For background simulation, we use an ‘MLM’ jet-matched [61, 62] cross-section for the inclusive for the W/Z +jets process with up to three additional jets. The $t\bar{t}$ channel uses a jet-matched cross-section for up to two additional jets. Other background channels are sub-leading and we only show-case their leading-order cross-sections. CMS has recently reported measurements on 13 TeV inclusive $t\bar{t}$ and W +jets channels. We adopt 746 pb [63] for $t\bar{t}$ production and 69 pb for W +jets production at $p_T^{j_1} \geq 100$ GeV [64]. Experimental measurements on the Z +jets channel [65] is more complicated to infer as it contains virtual photon contamination. We use the same measurement-to-simulation ratio as in W +jets to correct the Z +jets channel due to the kinematic similarity between the two channels.

Channel	tj	tW	$t\bar{t}$	W +jets	Z +jets	WWj	WZj	$M_N=100$	$M_N=110$
$\sigma(\mathbf{pb}), p_T^{j_1} > 200$ GeV	4.6	1.8	86	108	46	1.8	1.6	0.19	0.19
$\sigma(\mathbf{pb}), N_j \geq 3, N_l = 1$	0.34	0.24	18	4.9	0.54	0.25	0.16	0.39	0.48
$\sigma(\mathbf{fb}), M(j_2 j_3)$ on M_W	40	38	2.6×10^3	76	78	74	54	10	13
$\sigma(\mathbf{fb}), M_T \& M_{ljj} - 100 < 20$	5.5	1.0	63	23	4.4	4.0	1.4	8.0	—
$\sigma(\mathbf{fb}), M_T \& M_{ljj} - 110 < 20$	5.5	4.2	101	34	6.9	5.0	2.7	—	10

TABLE I: The SM background (left) and signal (right) cross-sections after selection cuts 1-3 (upper), and after selection cuts (4-5) with different M_N windows (lower). The inclusive cross-sections for $t\bar{t}$ and W/Z +jets are corrected to recent 13 TeV measurements. Other background channels are sub-leading and given at their lowest order. The signal cross-section is at LO and is given without the Higgs decay branching ratio, i.e. $\sigma_{\text{sig.}}/\mathcal{B}_{h \rightarrow N\nu}$, as a model independent result. The signal cross-section with $M_N = 100$ and 110 GeV assume a maximal mixing parameter at $|V_{lN}|^2 = 3.9 \times 10^{-4}$ and 6.3×10^{-4} , respectively.

The significant background channels are listed in Tab. I that shows the efficiency flow of the event selection cuts. For signal rates, we list two benchmark N masses at 100 and 110 GeV that optimize these selection efficiencies. Lower N masses would observe a reduced selection efficiency due to softer lepton energy and/or lower rate in reconstruction of a physical W mass.

We found the a residue total background cross-section of 0.1-0.16 pb. For a generic estimate with $\mathcal{B}_{h \rightarrow N\nu}$ at $\{5\%, 3\%, 1\%\}$ at future LHC with 3000 fb^{-1} luminosity, the sensitivity $S/\sqrt{S+B}$ is $\{2.1, 1.3, 0.4\}$ and $\{2.2, 1.3, 0.4\}$ for $M_N = 100$ GeV and $M_N = 110$ GeV. This sensitivity may improve by including NLO signal contribution in future studies. Note our selection cuts (1-5), in particular the leading jet trigger, are based on the current LHC design. For now we will assume similar trigger and cuts to estimate the sensitivity for future high luminosity. These cuts can be further optimized in case design upgrades become available.

In the 100-110 GeV mass range, this upper limit on $|V_{\ell N}|^2$ is dominated by leptonic Higgs search from LHC and it is M_N dependent. EWPD is most stringent in the $M_N < 100$ GeV range. The $|V_{\ell N}|^2$ bound assume flavor-blind coupling to all three lepton generations. We only consider the first two lepton generations and do not include the tau lepton channel due to lower tagging efficiency, plus the fact that only a fraction of the tau energy is visible. Both $h \rightarrow N_\mu \nu_\mu, N_e \nu_e$ channels contribute equally to our search. By Eq. 10 the corresponding total $\mathcal{B}_{h \rightarrow N\nu}$ in the FD case of the inverse seesaw model is 4% and 3% for $M_N = 100$ and 110 GeV. The LO sensitivity $S/\sqrt{S+B}$ at 3000 fb⁻¹ luminosity will be 1.7 at $M_N = 100$ GeV, and 1.3 at $M_N = 110$ GeV.

V. CONCLUSION

We investigated the prospects of probing the single-production of a heavy RHN from the on-shell decay of the SM Higgs boson at the LHC at 13 TeV. In the framework of the inverse see-saw model, a sizable neutrino mixing angle can be allowed. Due to the small decay width of the SM Higgs boson, a significant $h \rightarrow N\nu$ branching fraction can be allowed within the current bounds on the $N\nu$ mixing.

We adopt the $pp \rightarrow hj$ process as the search channel where the SM Higgs boson decays into the RHN followed by $N \rightarrow W\ell$ and $W \rightarrow jj$. One high p_T associated jet is required for triggering and also to transversely boost h decay products as well as better background suppression. A leading order calculation of the $pp \rightarrow hj$ process is carried out at one-loop level in signal event generation. The N mass is reconstructed in $N \rightarrow \ell W$, followed by $W \rightarrow q\bar{q}'$. A transverse mass cut is further introduced to reduce the SM $t\bar{t}, W$ +jets contributions.

We found a selection efficiency at 1-3% for M_N close to the Higgs boson mass and a reduced efficiency for lighter N . For a few benchmark N masses at 100 and 110 GeV, a leading order signal cross-section seems to be sub-fb after relevant selection requirements, compared with a total background of 0.1-0.16 pb. The significance at 2σ can be achieved at 3000 fb⁻¹ runs for a 5% branching ratio for $h \rightarrow N\nu$ decay. At the maximally allowed $N\nu$ mixing angle, the inverse model gives 4% and 3% at $h \rightarrow N\nu$ branching ratio and 1.7σ and 1.3σ signal significance at 3000 fb⁻¹. Note $pp \rightarrow hj$ is a QCD dominated process and future NLO calculations may enhance these significance prospects.

Acknowledgments

The work AD is supported by the Korea Neutrino Research Center which is established by the National Research Foundation of Korea(NRF) grant funded by the Korea government(MSIP) (No. 2009-0083526). YG is supported by the Institute of High Energy Physics, CAS, under the grant# Y7515560U1. YG also thanks the Wayne State University for support. TK is partially supported by DOE Grant de-sc0010813. TK is also supported in part by Qatar National Research Fund under project NPRP 9-328-1-066.

-
- [1] K. Nakamura *et al.* [Particle Data Group Collaboration], “Review of particle physics,” *J. Phys. G G* **37**, 075021 (2010).
 - [2] K. Abe *et al.* [T2K Collaboration] *Phys. Rev. Lett.* **107**, 041801 (2011).
 - [3] P. Adamson *et al.* [MINOS Collaboration], *Phys. Rev. Lett.* **107**, 181802 (2011).
 - [4] J. Beringer *et al.* [Particle Data Group Collaboration], *Phys. Rev. D* **86**, 010001 (2012).
 - [5] Y. Abe *et al.* [DOUBLE-CHOOZ Collaboration], *Phys. Rev. Lett.* **108**, 131801 (2012).
 - [6] F. P. An *et al.* [DAYA-BAY Collaboration], *Phys. Rev. Lett.* **108**, 171803 (2012).
 - [7] J. K. Ahn *et al.* [RENO Collaboration], *Phys. Rev. Lett.* **108**, 191802 (2012).
 - [8] P. Minkowski, “ $\mu \rightarrow e\gamma$ at a Rate of One Out of 10^9 Muon Decays?,” *Phys. Lett.* **67B**, 421 (1977). doi:10.1016/0370-2693(77)90435-X
 - [9] T. Yanagida, “Horizontal Symmetry and Masses of Neutrinos,” *Prog. Theor. Phys.* **64**, 1103 (1980).
 - [10] J. Schechter and J. W. F. Valle, “Neutrino Masses in $SU(2) \otimes U(1)$ Theories,” *Phys. Rev. D* **22**, 2227 (1980).
 - [11] T. Yanagida, in Proceedings of the Workshop on the Unified Theory and the Baryon Number in the Universe (O. Sawada and A. Sugamoto, eds.), KEK, Tsukuba, Japan, 1979, p. 95.
 - [12] M. Gell-Mann, P. Ramond, and R. Slansky, *Supergravity* (P. van Nieuwenhuizen *et al.* eds.), North Holland, Amsterdam, 1979, p. 315.
 - [13] S. L. Glashow, The future of elementary particle physics, in Proceedings of the 1979 Cargèse Summer Institute on Quarks and Leptons (M. Levy *et al.* eds.), Plenum Press, New York, 1980, p. 687.
 - [14] R. N. Mohapatra and G. Senjanovic, “Neutrino Mass and Spontaneous Parity Violation,” *Phys. Rev. Lett.* **44**, 912 (1980).
 - [15] R. N. Mohapatra, *Phys. Rev. Lett.* **56** (1986) 561.

- [16] R. N. Mohapatra and J. W. F. Valle, Phys. Rev. D **34**, 1642 (1986).
- [17] F. del Aguila and J. A. Aguilar-Saavedra, “Distinguishing seesaw models at LHC with multi-lepton signals,” Nucl. Phys. B **813**, 22 (2009) doi:10.1016/j.nuclphysb.2008.12.029 [arXiv:0808.2468 [hep-ph]].
- [18] M. Malinsky, T. Ohlsson, Z. z. Xing and H. Zhang, “Non-unitary neutrino mixing and CP violation in the minimal inverse seesaw model,” Phys. Lett. B **679**, 242 (2009) doi:10.1016/j.physletb.2009.07.038 [arXiv:0905.2889 [hep-ph]].
- [19] I. Garg, S. Goswami, Vishnudath K.N. and N. Khan, “Electroweak vacuum stability in presence of singlet scalar dark matter in TeV scale seesaw models,” Phys. Rev. D **96**, no. 5, 055020 (2017) doi:10.1103/PhysRevD.96.055020 [arXiv:1706.08851 [hep-ph]].
- [20] G. 't Hooft, “Naturalness, chiral symmetry, and spontaneous chiral symmetry breaking,” NATO Sci. Ser. B **59**, 135 (1980). doi:10.1007/978-1-4684-7571-5-9
- [21] A. Abada and M. Lucente, “Looking for the minimal inverse seesaw realisation,” Nucl. Phys. B **885**, 651 (2014) doi:10.1016/j.nuclphysb.2014.06.003 [arXiv:1401.1507 [hep-ph]].
- [22] I. Gogoladze, N. Okada and Q. Shafi, “NMSSM and Seesaw Physics at LHC,” Phys. Lett. B **672**, 235 (2009) doi:10.1016/j.physletb.2008.12.068 [arXiv:0809.0703 [hep-ph]].
- [23] A. Das and N. Okada, “Inverse seesaw neutrino signatures at the LHC and ILC,” Phys. Rev. D **88**, 113001 (2013) doi:10.1103/PhysRevD.88.113001 [arXiv:1207.3734 [hep-ph]].
- [24] A. Das, P. S. B. Dev and R. N. Mohapatra, “Same Sign vs Opposite Sign Dileptons as a Probe of Low Scale Seesaw Mechanisms,” arXiv:1709.06553 [hep-ph].
- [25] F. Deppisch and J. W. F. Valle, “Enhanced lepton flavor violation in the supersymmetric inverse seesaw model,” Phys. Rev. D **72**, 036001 (2005) doi:10.1103/PhysRevD.72.036001 [hep-ph/0406040].
- [26] A. Abada, D. Das, A. Vicente and C. Weiland, “Enhancing lepton flavour violation in the supersymmetric inverse seesaw beyond the dipole contribution,” JHEP **1209**, 015 (2012) doi:10.1007/JHEP09(2012)015 [arXiv:1206.6497 [hep-ph]].
- [27] A. Das, P. S. Bhupal Dev and N. Okada, “Direct bounds on electroweak scale pseudo-Dirac neutrinos from $\sqrt{s} = 8$ TeV LHC data,” Phys. Lett. B **735**, 364 (2014) doi:10.1016/j.physletb.2014.06.058 [arXiv:1405.0177 [hep-ph]].
- [28] P. S. Bhupal Dev, R. Franceschini and R. N. Mohapatra, “Bounds on TeV Seesaw Models from LHC Higgs boson Data,” Phys. Rev. D **86**, 093010 (2012) doi:10.1103/PhysRevD.86.093010 [arXiv:1207.2756 [hep-ph]].

- [29] M. Dittmar, A. Santamaria, M. C. Gonzalez-Garcia and J. W. F. Valle, “Production Mechanisms and Signatures of Isosinglet Neutral Heavy Leptons in Z^0 Decays,” Nucl. Phys. B **332**, 1 (1990). doi:10.1016/0550-3213(90)90028-C
- [30] S. Banerjee, P. S. B. Dev, A. Ibarra, T. Mandal and M. Mitra, “Prospects of Heavy Neutrino Searches at Future Lepton Colliders,” Phys. Rev. D **92**, 075002 (2015) doi:10.1103/PhysRevD.92.075002 [arXiv:1503.05491 [hep-ph]].
- [31] A. Das, P. Konar and S. Majhi, “Production of Heavy neutrino in next-to-leading order QCD at the LHC and beyond,” JHEP **1606**, 019 (2016) doi:10.1007/JHEP06(2016)019 [arXiv:1604.00608 [hep-ph]].
- [32] C. G. Cely, A. Ibarra, E. Molinaro and S. T. Petcov, “Higgs Decays in the Low Scale Type I See-Saw Model,” Phys. Lett. B **718**, 957 (2013) doi:10.1016/j.physletb.2012.11.026 [arXiv:1208.3654 [hep-ph]].
- [33] A. G. Hessler, A. Ibarra, E. Molinaro and S. Vogl, “Impact of the Higgs boson on the production of exotic particles at the LHC,” Phys. Rev. D **91**, no. 11, 115004 (2015) doi:10.1103/PhysRevD.91.115004 [arXiv:1408.0983 [hep-ph]].
- [34] A. M. Gago, P. Hernandez, J. Jones-Perez, M. Losada and A. Moreno Briceno, “Probing the Type I Seesaw Mechanism with Displaced Vertices at the LHC,” Eur. Phys. J. C **75**, no. 10, 470 (2015) doi:10.1140/epjc/s10052-015-3693-1 [arXiv:1505.05880 [hep-ph]].
- [35] O. Adriani *et al.* [L3 Collaboration], “Search for isosinglet neutral heavy leptons in Z^0 decays,” Phys. Lett. B **295**, 371 (1992). doi:10.1016/0370-2693(92)91579-X
- [36] M. Acciarri *et al.* [L3 Collaboration], “Search for heavy isosinglet neutrinos in e^+e^- annihilation at 130-GeV less than $S^{(1/2)}$ less than 189-GeV,” Phys. Lett. B **461**, 397 (1999) doi:10.1016/S0370-2693(99)00852-7 [hep-ex/9909006].
- [37] P. Achard *et al.* [L3 Collaboration], “Search for heavy isosinglet neutrino in e^+e^- annihilation at LEP,” Phys. Lett. B **517**, 67 (2001) doi:10.1016/S0370-2693(01)00993-5 [hep-ex/0107014].
- [38] P. Abreu *et al.* [DELPHI Collaboration], “Search for neutral heavy leptons produced in Z decays,” Z. Phys. C **74**, 57 (1997) Erratum: [Z. Phys. C **75**, 580 (1997)]. doi:10.1007/s002880050370
- [39] E. Fernandez-Martinez, J. Hernandez-Garcia and J. Lopez-Pavon, “Global constraints on heavy neutrino mixing,” JHEP **1608**, 033 (2016) doi:10.1007/JHEP08(2016)033 [arXiv:1605.08774 [hep-ph]].
- [40] J. de Blas, “Electroweak limits on physics beyond the Standard Model,” EPJ Web Conf. **60**,

- 19008 (2013) doi:10.1051/epjconf/20136019008 [arXiv:1307.6173 [hep-ph]].
- [41] F. del Aguila, J. de Blas and M. Perez-Victoria, “Effects of new leptons in Electroweak Precision Data,” *Phys. Rev. D* **78**, 013010 (2008) doi:10.1103/PhysRevD.78.013010 [arXiv:0803.4008 [hep-ph]].
- [42] E. Akhmedov, A. Kartavtsev, M. Lindner, L. Michaels and J. Smirnov, “Improving Electro-Weak Fits with TeV-scale Sterile Neutrinos,” *JHEP* **1305**, 081 (2013) doi:10.1007/JHEP05(2013)081 [arXiv:1302.1872 [hep-ph]].
- [43] F. F. Deppisch, P. S. Bhupal Dev and A. Pilaftsis, “Neutrinos and Collider Physics,” *New J. Phys.* **17**, no. 7, 075019 (2015) doi:10.1088/1367-2630/17/7/075019 [arXiv:1502.06541 [hep-ph]].
- [44] A. Das and N. Okada, “Bounds on heavy Majorana neutrinos in type-I seesaw and implications for collider searches,” arXiv:1702.04668 [hep-ph].
- [45] S. Chatrchyan *et al.* [CMS Collaboration], “Search for the standard model Higgs boson decaying to W^+W^- in the fully leptonic final state in pp collisions at $\sqrt{s} = 7$ TeV,” *Phys. Lett. B* **710**, 91 (2012) doi:10.1016/j.physletb.2012.02.076 [arXiv:1202.1489 [hep-ex]].
- [46] CMS Collaboration [CMS Collaboration], “Search for the standard model Higgs boson decaying to a W pair in the fully leptonic final state in pp collisions at $\sqrt{s} = 8$ TeV,” CMS-PAS-HIG-12-017.
- [47] G. Aad *et al.* [ATLAS Collaboration], “Search for the Standard Model Higgs boson in the $H \rightarrow WW^* \rightarrow \ell\nu\ell\nu$ decay mode with 4.7 /fb of ATLAS data at $\sqrt{s} = 7$ TeV,” *Phys. Lett. B* **716**, 62 (2012) doi:10.1016/j.physletb.2012.08.010 [arXiv:1206.0756 [hep-ex]].
- [48] S. Chatrchyan *et al.* [CMS Collaboration], “Search for the standard model Higgs boson in the H to ZZ to $2\ell 2\nu$ channel in pp collisions at $\sqrt{s} = 7$ TeV,” *JHEP* **1203**, 040 (2012) doi:10.1007/JHEP03(2012)040 [arXiv:1202.3478 [hep-ex]].
- [49] G. Aad *et al.* [ATLAS Collaboration], “Search for a standard model Higgs boson in the $H \rightarrow ZZ \rightarrow \ell^+\ell^-\nu\bar{\nu}$ decay channel using 4.7 fb $^{-1}$ of $\sqrt{s} = 7$ TeV data with the ATLAS detector,” *Phys. Lett. B* **717**, 29 (2012) doi:10.1016/j.physletb.2012.09.016 [arXiv:1205.6744 [hep-ex]].
- [50] [ATLAS Collaboration], “Search for Majorana neutrino production in pp collisions at $\sqrt{s} = 7$ TeV in dimuon final states with the ATLAS detector,” ATLAS-CONF-2012-139; S. Chatrchyan *et al.* [CMS Collaboration], “Search for heavy Majorana neutrinos in $\mu^\pm\mu^\pm +$ jets and $e^\pm e^\pm +$ jets events in pp collisions at $\sqrt{s} = 7$ TeV,” *Phys. Lett. B* **717**, 109 (2012) doi:10.1016/j.physletb.2012.09.012 [arXiv:1207.6079 [hep-ex]].

- [51] G. Aad *et al.* [ATLAS Collaboration], ‘Search for heavy Majorana neutrinos with the ATLAS detector in pp collisions at $\sqrt{s} = 8$ TeV,’ JHEP **1507** (2015) 162 doi:10.1007/JHEP07(2015)162 [arXiv:1506.06020 [hep-ex]].
- [52] V. Khachatryan *et al.* [CMS Collaboration], ‘Search for heavy Majorana neutrinos in $e^\pm e^\pm +$ jets and $e^\pm \mu^\pm +$ jets events in proton-proton collisions at $\sqrt{s} = 8$ TeV,’ JHEP **1604**, 169 (2016) doi:10.1007/JHEP04(2016)169 [arXiv:1603.02248 [hep-ex]].
- [53] A. Das and N. Okada, ‘Improved bounds on the heavy neutrino productions at the LHC,’ Phys. Rev. D **93**, no. 3, 033003 (2016) doi:10.1103/PhysRevD.93.033003 [arXiv:1510.04790 [hep-ph]].
- [54] A. Das, ‘Pair production of heavy neutrinos in next-to-leading order QCD at the hadron colliders in the inverse seesaw framework,’ arXiv:1701.04946 [hep-ph].
- [55] A. M. Sirunyan *et al.* [CMS Collaboration], ‘Search for heavy Majorana neutrinos in same-sign dilepton channels in proton-proton collisions at $\sqrt{s} = 13$ TeV,’ arXiv:1806.10905 [hep-ex].
- [56] A. M. Sirunyan *et al.* [CMS Collaboration], ‘Search for heavy neutral leptons in events with three charged leptons in proton-proton collisions at $\sqrt{s} = 13$ TeV,’ Phys. Rev. Lett. **120**, no. 22, 221801 (2018) doi:10.1103/PhysRevLett.120.221801 [arXiv:1802.02965 [hep-ex]].
- [57] M. Cacciari and G. P. Salam, ‘Pileup subtraction using jet areas,’ Phys. Lett. B **659**, 119 (2008) doi:10.1016/j.physletb.2007.09.077 [arXiv:0707.1378 [hep-ph]].
- [58] A. Das, P. S. B. Dev and C. S. Kim, ‘Constraining Sterile Neutrinos from Precision Higgs Data,’ Phys. Rev. D **95**, no. 11, 115013 (2017) doi:10.1103/PhysRevD.95.115013 [arXiv:1704.00880 [hep-ph]].
- [59] C. O. Dib, C. S. Kim, K. Wang and J. Zhang, ‘Distinguishing Dirac/Majorana Sterile Neutrinos at the LHC,’ Phys. Rev. D **94**, no. 1, 013005 (2016) doi:10.1103/PhysRevD.94.013005 [arXiv:1605.01123 [hep-ph]].
- [60] J. Alwall *et al.*, ‘The automated computation of tree-level and next-to-leading order differential cross sections, and their matching to parton shower simulations,’ JHEP **1407**, 079 (2014) doi:10.1007/JHEP07(2014)079 [arXiv:1405.0301 [hep-ph]].
- [61] S. Mrenna and P. Richardson, ‘Matching matrix elements and parton showers with HERWIG and PYTHIA,’ JHEP **0405**, 040 (2004) doi:10.1088/1126-6708/2004/05/040
- [62] M. L. Mangano, M. Moretti, F. Piccinini and M. Treccani, ‘Matching matrix elements and shower evolution for top-quark production in hadronic collisions,’ JHEP **0701**, 013 (2007) doi:10.1088/1126-6708/2007/01/013 [hep-ph/0611129].

- [63] A. M. Sirunyan *et al.* [CMS Collaboration], “Measurement of normalized differential t-tbar cross sections in the dilepton channel from pp collisions at $\sqrt{s} = 13$ TeV,” arXiv:1708.07638 [hep-ex].
- [64] A. M. Sirunyan *et al.* [CMS Collaboration], “Measurement of the differential cross sections for the associated production of a W boson and jets in proton-proton collisions at $\sqrt{s} = 13$ TeV,” Phys. Rev. D **96**, no. 7, 072005 (2017) doi:10.1103/PhysRevD.96.072005 [arXiv:1707.05979 [hep-ex]].
- [65] M. Aaboud *et al.* [ATLAS Collaboration], “Measurements of the production cross section of a Z boson in association with jets in pp collisions at $\sqrt{s} = 13$ TeV with the ATLAS detector,” Eur. Phys. J. C **77**, no. 6, 361 (2017) doi:10.1140/epjc/s10052-017-4900-z [arXiv:1702.05725 [hep-ex]].